Progress In Electromagnetics Research, PIER 98, 53–73, 2009

THE DEVELOPMENT OF CURVED MICROSTRIP ANTENNA WITH DEFECTED GROUND STRUCTURE

J. P. Geng, J. J. Li, R. H. Jin, S. Ye, X. L. Liang and M. Z. Li

Department of Electronic Engineering
Shanghai Jiao Tong University
Shanghai 200240, China

Abstract—A series of curved microstrip antennae with defected ground structure for multiband are proposed, which are more smaller, conveniently conformal, wider radiation beam and suitable for WLAN terminal for different environment. The relation between the main geometry parameters and the antennas' characters are studied with the cavity model method and EM simulation, and the optimum size antenna is achieved later. If keeping the other parameters but increasing the curving angle α, the return loss is almost good at $f = 2.45\,\text{GHz}$, but poor at $f = 5.25\,\text{GHz}$ and $5.8\,\text{GHz}$. After slight tuning the key parameters, these curved antennae all can work at $f = 2.45\,\text{GHz}$, $5.25\,\text{GHz}$ and $5.8\,\text{GHz}$, and their patterns in the plane that is vertical to the curve axes become more wider or even omni-directional with the curving angle α increasing, which are verified by experiment, their measured gain are $2\,\text{dB}$–$6.3\,\text{dB}$.

1. INTRODUCTION

With the fast development of wireless communication, the small multi-function terminal with multi-frequency bands has attracted considerable interests of users, but the RF module and antenna still occupy more than 60% size of the terminal at present, how to reduce the dimension of the antenna in the terminal has been very critical. In one side, the antenna should be small enough to be integrated into the terminal; in another side, the work band of the antenna should cover several effective frequency bands with high gain, omni-directional or directional pattern, being conformal easily. For example, the simple solution for WLAN terminal antenna is the external monopoles for

Corresponding author: J. P. Geng (gengjunp@sjtu.edu.cn).

2.4 GHz, 5.25 GHz or 5.8 GHz, but it is unsightly and incident to be damaged. The microstrip antenna, slot antenna, printed antenna with several branches or their array are another choice for WLAN [1–6] because of low profile, low cost, lightweight and conveniently to be integrated with RF devices.

Conformal microstrip antennas are applied for a wide variety of higher frequency, such as the cylindrical microstrip antenna, has been paid more attention by many researchers [7–9], which can reduce the size, widen the radiation beam. The surface wave restricts the wide use of microstrip antenna, electromagnetic bandgap (EBG) or photonic bandgap (PBG) structure is a method to reduce the surface waves, which exhibit band-gap feature [10] too. EBG has been applied in the field of antenna to improve the performance of antenna [11–16], such as suppression of surface wave propagation, increasing the gain of antenna and improving the radiation pattern by inserting the EBG structure into the substrate [17–19]. However, in implementing EBG, a large area is needed to implement the periodic patterns and it is also difficult to define the unit element of EBG. Whereas the defected ground structure (DGS) has similar microwave circuit properties as EBG, it can also modify guided wave properties to provide a bandpass or bandstop like filter and can easily define the unit element. DGS is realized by etching the ground plane of microstrip antenna, this disturbs the shield current distribution in the ground plane which influences the input impedance and current flow of the antenna. The geometry of DGS can be one or few etched structure which is simpler and does not need a large area to implement it [20]. Many shapes of DGS slot have been studied in planar microsrip antenna designs [21–23], which provides many good performances — size reduction (resonant frequency lower), impedance bandwidth enhancement (quality factor lower) and gain increasing. In [24], the compact, broadband microstrip antenna with defective ground plane has bee realized, the impedance bandwidth of the proposed antenna could reach about 4.3 times that of the conventional microstrip antenna. In [22], several slots are embedded in the ground of the microstrip antenna so that the size is reduced, the impedance band and gain is enhanced. In [25], utilizing a slot-load technique, the microstrip slot antenna excites two remnant frequencies. By combining with a defective ground plane, the bandwidth is augmented and the resonant frequency is lowed simultaneously. What's more, one dimensional defected ground structure (DGS) is used to eliminates the second and third harmonics and improves the return loss level, and decreases the occupied area by 70% compared to the conventional,

In this paper, the DGS is adopted in the ground design of the microstrip antenna to achieve the useful multiband, small size and

high gain, and a series of curved cylindrical antennas with DGS for multiband are proposed, which are more smaller, wider radiarion beam and suitable for WLAN terminal for different radiation environment. Firstly, the planar microstrip antennas with DGS on the limited ground is studied. The optimized result is manufactured, which show good performance for the triple frequency 2.45 GHz, 5.25 GHz and 5.8 GHz. Based on the results of planar antennas, a series of curved conformal antennae with different curving angle α are designed and fabricated. The impact on resonance frequencies and radiation patterns brought by curving the antennae are explored and summarized by simulations and measured results.

2. GEOMETRY STRUCTURE AND ANALYSIS METHOD

2.1. Antenna Geometry with Defected Ground

The basic geometry is the rectangular patch antenna, which is shown in Fig. 1(a). The rectangular patch is in one side (size: length1 $\times$ length2), and the ground with several rectangular holes is in another side (Fig. 1(b)), the detail parameters are shown in Fig. 1.

In fact, the patch in the front side of the planar antenna can resonate in two polarization models by current distribution: U direction current and V direction current, if the ground is a whole rectangular conductor plane. Here the actual ground is conductor plane with holes, and the patch size is smaller than the maximum size of the ground, so that the patch can still work in two polarization models.

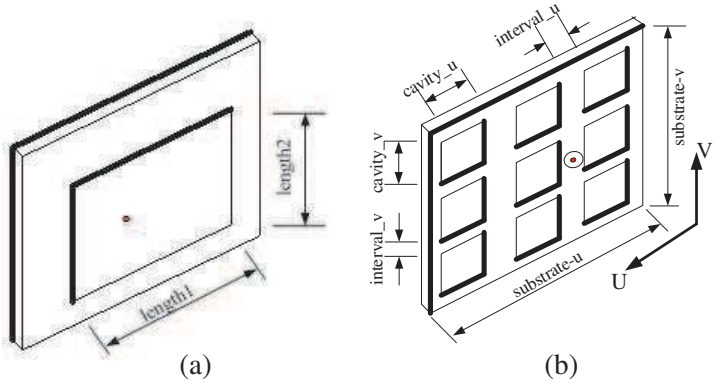

Figure 1. The rectangular patch antenna with DGS: (a) Front side; (b) Back side.

In Fig. 1(b), the actual ground is conductor plane with several rectangular holes, which is the defected ground structure (DGS) with frequency selective characters, and the hole size decides some working frequency band [26].

When the rectangular patch and the ground with rectangular holes are combined, the frequency band of the patch is filtered by the DGS, so that result in several available bands.

The curved antenna is shown in Fig. 2, which almost keep the size same as those in Fig. 1, only the curving angle α is different, the curving axis is parallel with Z axis in Fig. 2.

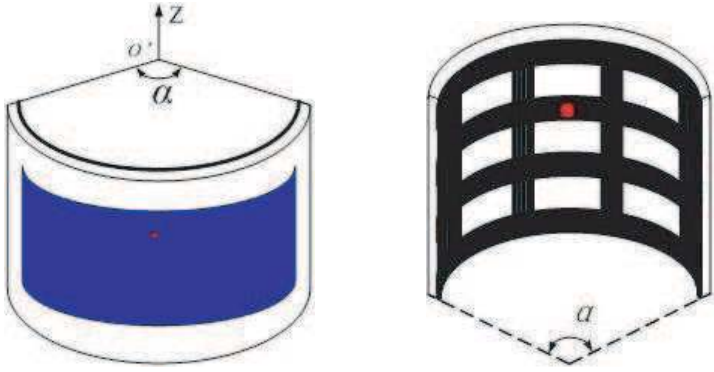

(a) (b)

Figure 2. The curved rectangular antenna, the curving angle is α. (a) front side; (b) back side.

2.2. Equivalent Circuit

According to the cavity model, the general topology of the wideband lumped equivalent circuit of rectangular microstrip antenna can be determined as shown in Fig. 3 by applying the modified mode expansion technique to the advanced cavity model of rectangular microstrip patch antenna [27, 28]

From Fig. 3, the equivalent impedance $Z_{eq}(f)$ of the patch antenna can be written as:

$$Z_{eq}(f) = j2\pi f L_{\infty} + \frac{1}{j2\pi f C_{0,0}} + \sum_{i=1}^{M} \frac{R_{0,i}}{1 + jQ_{0,i}\left(\frac{f}{f_{0,i}} - \frac{f_{0,i}}{f}\right)} \tag{1}$$

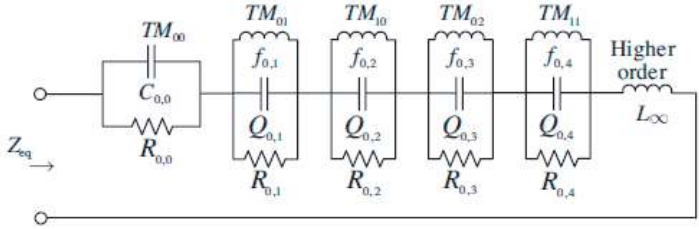

Figure 3. The equivalent circuit model to the rectangular microstrip patch antenna [28].

When the frequency $f \to 0$, Equation (1) will be simplified as

$$\lim_{f\to 0} Z_{eq}(f) = \lim_{f\to 0} \frac{1}{j2\pi f C_{0,0}} + jf\left(2\pi L_\infty + \sum_{i=1}^{M} \frac{R_{0,i}}{Q_{0,i} f_{0,i}}\right) = \frac{1}{j2\pi f C_{0,0}} \tag{2}$$

So, the capacitance C_{00} can be gotten by Equation (3)

$$\begin{aligned} C_{00} &\approx \lim_{f\to 0} \frac{1}{2\pi f^2 \frac{\partial \mathrm{Im}[Zm(f)]}{\partial f}} \\ &\approx \frac{6\Delta f}{\pi f_3^2 \mathrm{Im}[Z_m(f_1) - 8Z_m(f_2) + 8Z_m(f_4) - Z_m(f_5)]} \end{aligned} \tag{3}$$

Similarly, when the frequency $f \to \infty$, Equation (1) will be simplified as

$$\lim_{f\to\infty} Z_{eq}(f) = j2\pi L_\infty f + \frac{1}{jf}\left(\frac{1}{2\pi C_{0,0}} + \sum_{i=1}^{M} \frac{R_{0,i} f_{0,i}}{Q_{0,i}}\right) = j2\pi L_\infty f \tag{4}$$

So, we get the inductance L_∞,

$$\begin{aligned} L_\infty &\approx \lim_{f\to\infty} \frac{\partial \mathrm{Im}[Z_m(f)]}{2\pi \partial f} \\ &\approx \frac{\mathrm{Im}[Z_m(f_{N-4}) - 8Z_m(f_{N-3}) + 8Z_m(f_{N-1}) - Z_m(f_N)]}{24\pi\Delta f} \end{aligned} \tag{5}$$

$$R_{0,i} \approx \mathrm{Re}[Z_m(f)]|_{f=f_{0,i}} \tag{6}$$

$$Q_{0,i} \approx -\frac{f_{0,i}}{2R_{0,i}} \times \mathrm{Im}\left[\frac{\partial Z_m(f)}{\partial f}\right]|_{f=f_{0,i}} \tag{7}$$

When the microstrip antenna is fed by the probe, the introduced impedance for some mode could be written as [29]

$$X_L = \frac{377h}{\lambda_0} \ln \frac{\lambda_0}{\pi d_0 \sqrt{\varepsilon_r}} \tag{8}$$

2.2.1. Planar Microstrip Antenna with DGS

When the DGS-several rectangular holes embedded in the ground of the planar microstrip antenna, some experiments results have shown the good performance of size reduction, impedance band and gain enhancement [21, 24, 25]. So, we can give some conclusion for DGS embedded in the ground:

(i) The DGS can be equivalent to a larger capacitance, which is available to reduce antenna size according to the transmission line theory.

(ii) According to [30], DGS structure result in slow-wave, which is equivalent to increase capacitance and inductance.

(ii) The rectangular holes in the ground increase the length of the current flowing distance, just like an additional inductance.

(iv) According to the cavity model, the antenna with DGS can be equivalent to the similar circuit, although the elements are different from the planar antenna without DGS.

(v) For higher frequency, the DGS can be equivalent to capacitance parallelly connected with inductance to form a new resonant frequency band to augment the original band [31].

(vi) The DGS in the ground reduces the surface wave to enhance the antenna gain.

So, the planar microstrip antenna with DGS ground can be approximately equivalent to the circuit in Fig. 3 too.

2.2.2. Curved Microstrip Antenna with Defected Ground Structure

When the curved radian is small, the equivalent circuit is almost same as the above.

When the curved radian is great, the capacitance and inductance may be affected by the mutual coupling, but the main principle is similar as the above.

2.3. Simulation Method and Experiment Condition

In the early, the transmission line model and the cavity model are used to analyze the microstrip antenna, Green function has been regarded as a precise full wave method to microstrip. Finite Integration in Time domain (FIT) is too.

Here, the electromagnetic numerical calculation tool is CST MICROWAVE STUDIO, which is based on Finite Integration in Time domain and Finite Difference in Time Domain methods [32, 33].

For the experiment, the Agilent vector network analyzer 8722ES is used to measure the return loss of the antenna. The pattern and gain of the experiment antennae are measured in an half open space-on the top of our lab building with signal generator Agilent PSG E8267D, spectrum analyzer Agilent PSA E4447A and the antenna rotator. The gain of the experiment antenna is estimated by comparing the experiment data with the standard horn antennas at the same frequencies [34].

3. RESULT ANALYSIS FOR PLANAR ANTENNA WITH DGS

Some original parameters of the planar antenna are given: ε_r of substrate is 2.02, substrate thickness is 2 mm, covered copper thickness is 0.018 mm, interval_u = interval_v = 3 mm, cavity_u = 10.8 mm, cavity_v = 11.7 mm, substrate_u = 45 mm, substrate_v = 47 mm, length1 = 35.5 mm, length2 = 39 mm. The antenna is fed by probe with 50 Ohm.

3.1. Impedance

Here, a microstrip antenna without DGS and another one with DGS are simulated, their external size are same as the above, and the impedance are compared in Fig. 4.

In Fig. 4, the impedance-frequency curves for the mircrostrip antenna with DGS and the antenna without DGS are similar, and the resonant frequency decrease clearly, which is in accordant with the assumption of the equivalent circuit of the antenna with DGS.

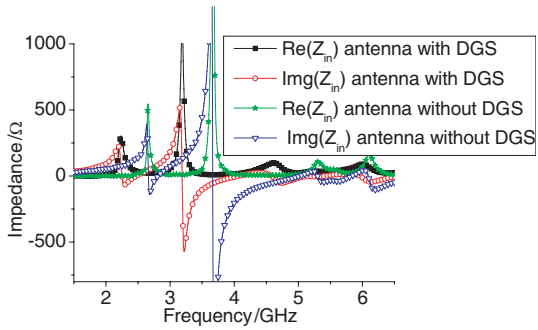

Figure 4. Input Impedance: real part and Imaginary part for same external size microstrip antenna without DGS and another one with DGS.

Table 1. The parameters of these working models for patch antenna without DGS and patch antenna with DGS.

		Patch (no DGS)	Patch (with DGS)
	C_{00} (pF)	17.08 pF	12.07 pF
	L_∞ (nH)	8.27 nH	13.45 nH
TM_{01}	f_{01} (GHz)	2.664	2.254 GHz
	R_{01} (Ω)	459.64	236.06
	Q_{01}	43.38	12.26
TM_{10}	f_{02} (GHz)	3.675 GHz	3.199 GHz
	R_{02} (Ω)	2609.0	1108.3
	Q_{02}	52.24	46.10
TM_{02}	f_{03} (GHz)	5.306 GHz	4.578 GHz
	R_{03} (Ω)	108.72	98.28
	Q_{03}	24.85	9.21
TM_{11}	f_{04} (GHz)	6.093 GHz	5.957
	R_{04} (Ω)	154.18	81.35
	Q_{04}	28.77	8.09

In another side, according to the cavity model, the parameters of these working models are calculated in the Table 1. These two antenna's working models are similar, so that the cavity model could still be used to analyze the patch antenna with DGS. For the patch antenna with DGS, TM_{01}, TM_{10}, TM_{02} and TM_{11} all move to the lower frequency, the C_{00} decrease, L_∞ increase, and their Q_{0i} become smaller too.

During the simulation, it is found that the length1, length2 and cavity_u are the sensitive parameters, so these parameters are discussed in the following in detail.

3.2. Length1

The length1's effect to the character of the basic plane patch antenna with DGS is studied in Fig. 5. The trough of the return loss $|S_{11}|$ move to lower band near 2.45 GHz, 5.25 GHz and 5.8 GHz with length1 increasing.

In details, the effect of length1 to the working models are listed in Table 2. With length1 increasing, the L_∞ increase rapidly, these 4 working models all are affected greatly, and they all move lower frequency.

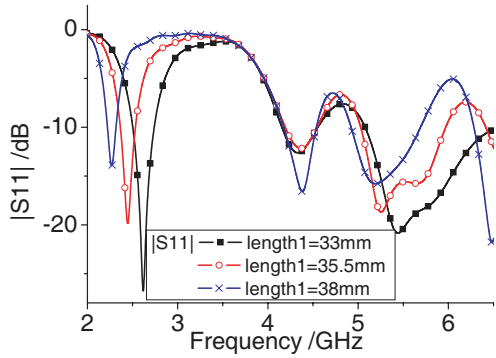

Figure 5. The length1's impact on all the resonance frequencies.

Table 2. The parameters of these 4 models for patch antenna with DGS with length1 varying.

length1 (mm)		33	35.5	38
C_{00} (pF)		10.69	11.03	12.13
L_∞ (nH)		9.03	17.54	20.48
TM_{01}	f_{01} (GHz)	2.338	2.24	2.121
	R_{01} (Ω)	270.45	276.00	306.4329
	Q_{01}	11.07	14.31	21.76
TM_{10}	f_{02} (GHz)	3.283	3.178	3.069
	R_{02} (Ω)	562.15	1253.55	1960.62
	Q_{02}	23	48.82	72.55
TM_{02}	f_{03} (GHz)	4.606	4.592	4.55
	R_{03} (Ω)	102.88	104.24	100.55
	Q_{03}	8.9	9.61	11.79
TM_{11}	f_{04} (GHz)	6.0836	5.943	5.754
	R_{04} (Ω)	74.29	91.65	107.63
	Q_{04}	6.82	10.24	11.28

3.3. Length2

The length2's effect to the return loss $|S_{11}|$ of the plane patch antenna with DGS is studied in Fig. 6. With length2 increasing from 42 mm to 48 mm, the trough of $|S_{11}|$ keep stable near 2.45 GHz, appear inflexion near 5.25 GHz, but shallow near 5.8 GHz.

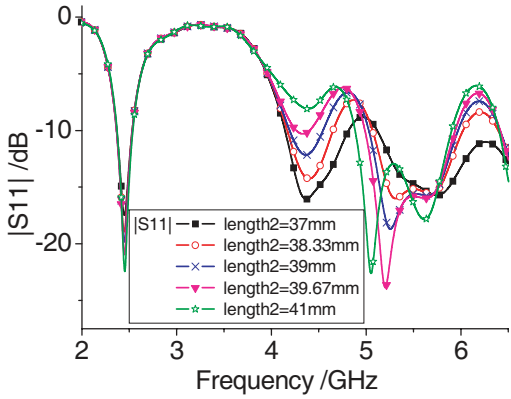

Figure 6. The length2's impact on all the resonance frequencies.

Table 3. The parameters of these 4 models for patch antenna with DGS with length2 varying.

Length2 (mm)		37 mm	38.33	39	39.67	41
C_{00} (pF)		10.64	10.89	11.03	11.17	11.67
L_{∞} (nH)		13.32	16.22	17.54	18.67	20.21
TM_{01}	f_{01} (GHz)	2.24	2.24	2.24	2.24	2.247
	R_{01} (Ω)	276.83	273.43	276.00	277.72	272.03
	Q_{01}	14.86	14.24	14.31	14.46	13.68
TM_{10}	f_{02} (GHz)	3.22	3.195	3.178	3.164	3.129
	R_{02} (Ω)	1268.26	1261.2	1253.55	1227.74	1196.35
	Q_{02}	49.11	52.74	48.82	47.83	49.48
TM_{02}	f_{03} (GHz)	4.494	4.592	4.592	4.575	4.49
	R_{03} (Ω)	71.65	87.3	104.24	117.94	121.56
	Q_{03}	4.39	5.92	9.61	11.91	10.23
TM_{11}	f_{04} (GHz)	6.027	5.971	5.943	5.926	5.894
	R_{04} (Ω)	79.45	89.27	91.65	93.2	94.34
	Q_{04}	8.05	10.18	10.24	10.5	11.21

In details, the effect of length2 to the working models are listed in Table 3. With length2 increasing from 37 mm to 41 mm, the C_{00} increase little, L_{∞} increase distinctly, The TM_{01}, TM_{10} and TM_{02} almost keep stable, but TM_{11} varies in evidently.

3.4. Cavity_u

The cavity_u's effect to the return loss $|S_{11}|$ of the plane patch antenna with DGS is studied in Fig. 7. With cavity_u increasing, the trough of $|S_{11}|$ become deeper near 2.45 GHz and 5.8 GHz, but shallow near 5.25 GHz.

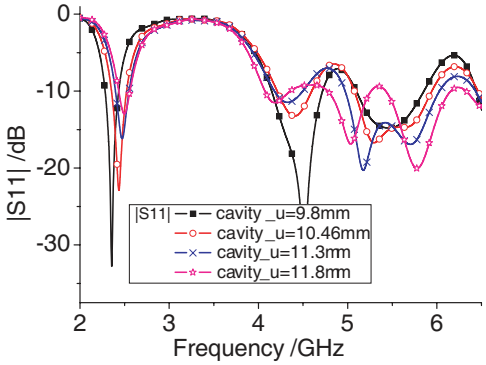

Figure 7. The cavity_u's impact on all the resonance frequencies.

Table 4. The parameters of these 4 models for patch antenna with DGS with cavity_u varying.

cavity_u (mm)		9.8	10.46	11.13	11.8
C_{00} (pF)		11.99	10.96	11.23	10.83
L_∞ (nH)		19.28	17.08	16.24	15.22
TM_{01}	f_{01} (GHz)	2.219	2.236	2.254	2.252
	R_{01} (Ω)	175.36	263.99	313.11	419.03
	Q_{01}	8.17	13.72	16.54	23.46
TM_{10}	f_{02} (GHz)	3.115	3.157	3.199	3.227
	R_{02} (Ω)	1329.46	1340.27	1138.45	1240.18
	Q_{02}	42.75	51.28	45.68	51.46
TM_{02}	f_{03} (GHz)	4.697	4.62	4.55	4.403
	R_{03} (Ω)	89.94	100.83	102.96	99.01
	Q_{03}	10.50	9.54	8.4	8.09
TM_{11}	f_{04} (GHz)	5.936	5.964	5.971	5.999
	R_{04} (Ω)	112.19	100.05	87.53	76.29
	Q_{04}	12.82	12.39	10.58	10.16

In details, the effect of cavity_u to the working models are listed in Table 4. With cavity_u increasing from 9.8 mm to 11.8 mm, the C_{00} almost keep stable, L_∞ decrease, the TM_{01}, TM_{10}, TM_{02} and TM_{11} all are affected.

3.5. The Final Parameters for the Plane Microstrip Antenna with DGS

From the above analysis, the final parameters of the antenna with are decided in the following, ε_r of substrate is 2.02, substrate thickness is 2 mm, covered copper thickness is 0.018 mm, interval_u = interval_v = 3 mm, cavity_u = 10.8 mm, cavity_v = 11.8 mm, substrate_u = 45 mm, substrate_v=47 mm, length1 = 35.5 mm, length2 = 39 mm. The antenna is fed by probe with 50 Ohm. The really fabricated plane antenna with DGS is shown in Fig. 8 (center angle $\alpha = 0°$). The simulated and measured return loss $|S_{11}|$ of the antennae with DGS are in Fig. 9 (center angle $\alpha = 0°$).

Figure 8. Curved antennas with different central angle α (0°, 45°, 90°, 135°, 180°, 225° and 270°) for experiment.

4. CURVED ANTENNAE

Based on the planar patch antenna with DGS in Fig. 8, the antenna is curved in different central angle α, which is suitable for the conformal and reduce size of the antenna. Just like in Fig. 2, the antenna is curved around the Z axis, and the curving angle α is set as 0°, 45°, 90°, 135°, 180°, 225° and 270°, the practical curved antennas are shown in Fig. 8, and these antenna's characters and their variance rule are studied by simulation and measurement, and the approximate cavity model are still used to analyze these curved antenna.

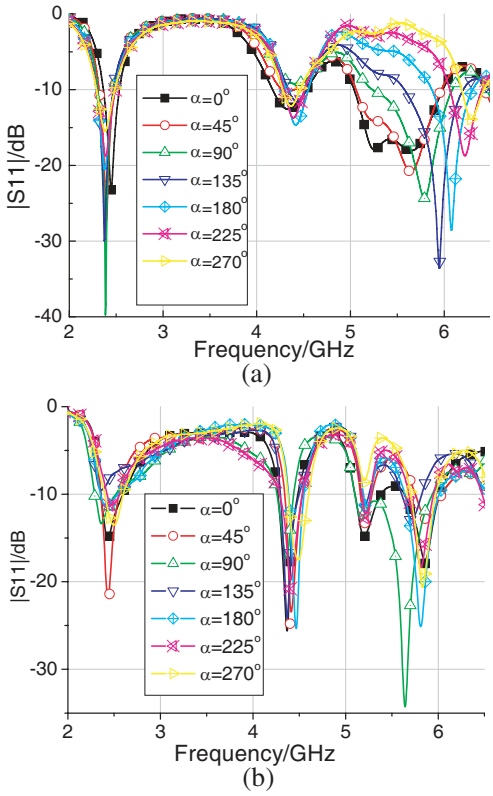

Figure 9. $|S_{11}|$ with different curving angle α: (a) simulation for curved antenna with original size; (b) measured $|S_{11}|$ for the curved antenna with refined parameter value.

4.1. The Curving Angle α Varies, But Other Parameters Are Kept

Keeping the parameters' value as the above, the planar antennas are curved in different central angle α, the simulated return loss $|S_{11}|$ are shown in Fig. 9(a). With the curving angle α increasing, the return loss $|S_{11}|$ almost keep stable at 2.45 GHz, but raise in $5.25 \sim 5.8$ GHz.

In the further, the effect of the curving angle α to the working models are listed in Table 5. With the curving angle α increasing from 0° to 270°, the C_{00} decrease slowly, L_∞ increase. When the curving angle α increase, the f_{03} moving toward right, and a new model appears at about 4.33 GHz, $\alpha = 225^\circ$, so that 5 working models exist during $2 \sim 6$ GHz.

After some parameters are refined slightly in manufacturing as shown in Table 6, and the counterpart measured $|S_{11}|$ are in Fig. 9(b).

With the curving angle α increasing, $|S_{11}|$ almost keep stable near 2.45 GHz, and $|S_{11}| < -10$ dB at 2.45 GHz, 5.25 GHz and 5.8 GHz, although these curves are different greatly.

In the further, the effect of the curving angle α to the working models of the refined curved antennas are listed in Table 5. There are 5 working models in these antennae during 2–6 GHz. With the curving angle α increasing from 0° to 270°, the C_{00} decrease slowly, L_∞ increase, the TM_{01}, TM_{10}, TM_{02}, TM_{11} and TM_{20} all are affected.

In another side, although the parameters' value of the original planar antennas are same, the parameters' value (along the circumferential direction) varies a little when the planar antennas are curved in different alpha. Assume the length of the arc (along the circumferential direction) is l, the thickness of the planar antenna is hd. Keeping the arc length l of the outside, and curving angle is α (degree), then the inside length will be shorter and the error of the inside length $\Delta l \leq 0$,

$$\Delta l = -hd \cdot \alpha \cdot \pi/180 \leq 0 \tag{9}$$

This's just why the valid frequency band 5.2–5.8 GHz will move right with the curving angle α increasing in Fig. 9(a).

Table 5. The parameters of the working models for the curved patch antenna with DGS with the curving angle α varying.

		curved antenna						refined curved antenna					
	α(°)	45°	90°	135°	180°	225°	270°	45°	90°	135°	180°	225°	270°
	C_{00} (pF)	11.68	11.63	11.45	11.3	11.25	11.16	11.81	11.76	11.73	11.76	11.19	11.36
	L_∞(nH)	17.21	15.67	16.67	15.88	15.98	8.313	23.14	20.07	24.78	35.98	42.8	23.40
TM 01	f_{01}(GHz)	2.24	2.247	2.254	2.282	2.205	2.205	2.24	2.219	2.198	2.107	2.58	2.114
	$R_{01}(\Omega)$	200.18	170.98	142.61	116.33	151.85	130.45	198.38	170.53	135.55	64.62	151.37	162.78
	Q_{01}	10.32	6.32	5.16	2.73	9.3	7.33	9.11	6.76	4.4	23.24	10.32	9.71
TM 10	f_{02}(GHz)	3.22	3.234	3.248	3.255	3.262	3.283	3.199	3.15	3.132	3.115	3.101	3.115
	$R_{02}(\Omega)$	1437.29	1197.64	1030.7	916.21	769.42	911.69	1389.46	1163.83	820.51	856.33	728.01	712.22
	Q_{02}	48.2	39.4	32.58	26.72	22.24	29.3	50.39	38.93	25.14	26.63	23.05	22.37
TM 02	f_{03}(GHz)	4.564	4.585	4.704	4.837	4.333	4.375	4.55	4.515	4.557	4.641	4.032	4.543
	$R_{03}(\Omega)$	109.37	113.28	148.16	307.55	30.83	35.25	147.18	252.73	354.94	253.99	29.99	205.15
	Q_{03}	7.61	7.96	14.04	44.69	8e-6	2.25	13.89	30.28	49.86	38.57	0.0005	33.80
TM 11	f_{04}(GHz)	———	———	———	———	4.949	5.033	5.173	5.082	5.005	4.963	4.963	5.082
	$R_{04}(\Omega)$	———	———	———	———	490.96	379.70	42.94	54.86	68.08	133.63	495.38	1118.20
	Q_{04}	———	———	———	———	72.04	52.15	2.813	6.12	6.37	19.06	62.98	136.7
TM 20	f_{05}(GHz)	5.87	5.894	5.999	6.111	6.265	6.398	5.803	5.831	5.789	5.775	5.838	5.873
	$R_{05}(\Omega)$	71.86	56.54	49.89	44.49	37.34	28.26	705	78.15	68.43	51.96	37.82	45.34
	Q_{05}	5.84	3.47	5.45	9.183	9.55	4.34	3.75	13.31	11.27	12.15	9.06	14.93

Table 6. Modified parameters of the curved antennas with different central angles.

Angle α (°)	0	45	90	135	180	225	270
cavity_u g(mm)	10.8	10.8	10.8	10.8	10.8	10.8	10.8
cavity_v (mm)	11.8	11.8	12	12.3	12.6	12.9	12
interval_u (mm)	3	3	3	3	3	3	3
interval_v (mm)	3	3	2.7	2.3	2.2	1.8	1.6
length1 (mm)	35.5	35.5	35.5	35.5	35.5	35.5	35.5
length2 (mm)	39	40	42	42.8	43	43.4	44
substrate_u (mm)	45	45	45	45	45	45	45
substrate_v (mm)	47	47	47	47	47	47	47

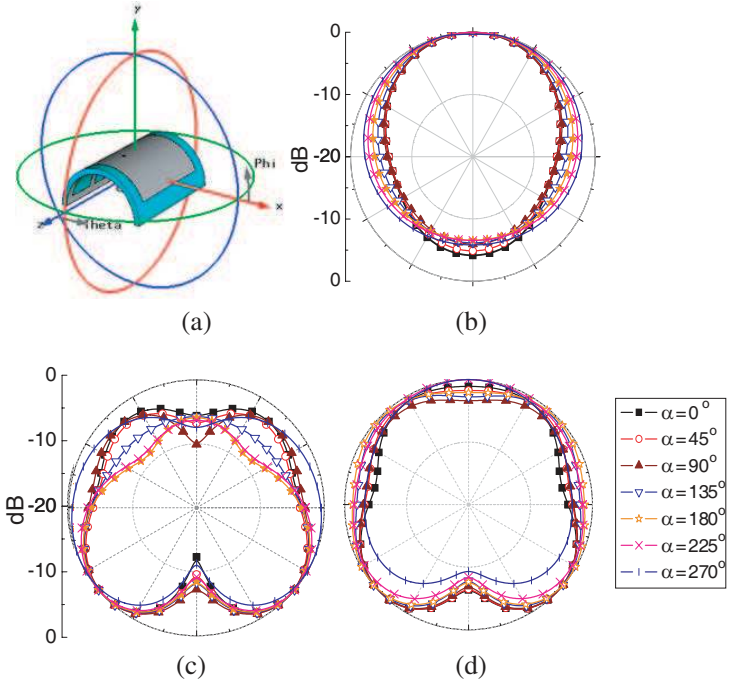

Figure 10. Curved conformal antennas' simulation pattern in XY plane for the different curving angle α: (a) Coordinate system; (b) $f = 2.45\,\text{GHz}$; (c) $f = 5.25\,\text{GHz}$; (d) $f = 5.8\,\text{GHz}$.

Refer to result of Fig. 6 in Part 3, the valid frequency band 5.2–5.8 GHz moved left with lenth2 increasing. So, length2 is increased in Table 6 with α increasing to keep the valid frequency band 5.2–5.8 GHz (in Fig. 9(b)).

Other parameters are adjusted slightly in Table 6 to match the impedance validly.

4.2. Patten Varying with the Curving Angle α

Assume the coordinate of the curved antenna is same as in Fig. 10(a).

Based on the parameter's value in Table 3, the simulated patterns at 2.45 GHz, 5.25 GHz and 5.8 GHz with different the curving angle α are shown in Fig. 10.

In Fig. 10(b), the radiation beam in XY plane become wider with the curving angle α increasing at 2.45 GHz, when $\alpha = 270°$, the half band beam width is even more than 180°.

In Fig. 10(c), the radiation beam in XY plane become wider with the curving angle α increasing at 5.25 GHz, but two zero points appear in y direction and $-y$ direction.

In Fig. 10(d), the radiation beam in XY plane become wider with the curving angle α increasing at 5.8 GHz, but there is one zero point in $-y$ direction. When $\alpha = 270°$, the half band beam width is even more than 180°.

The measured patterns for these curved antennae are achieved in half open space on the top of our lab building, which are shown in Fig. 11, and the measured patterns are similar with the simulated results, although there are some difference between them, which verified that the simulated results of the radiation beam in XY plane will become wider when the curving angle α increases.

Table 7. Antenna gain (dBi).

f (GHz) / α (°)	Simulated			Measured		
	2.45	5.25	5.8	2.45	5.25	5.8
0	5.224	5.129	2.84	5.815	4.485	3.583
45	5.501	4.106	3.297	4.905	4.568	2.577
90	5.421	5.297	3.934	6.305	3.843	3.826
135	5.306	3.509	4.423	5.075	4.376	4.027
180	4.993	3.311	3.744	5.375	3.038	2.206
225	4.631	3.314	3.666	4.815	3.242	3.718
270	4.254	3.467	3.852	3.805	4.342	4.804

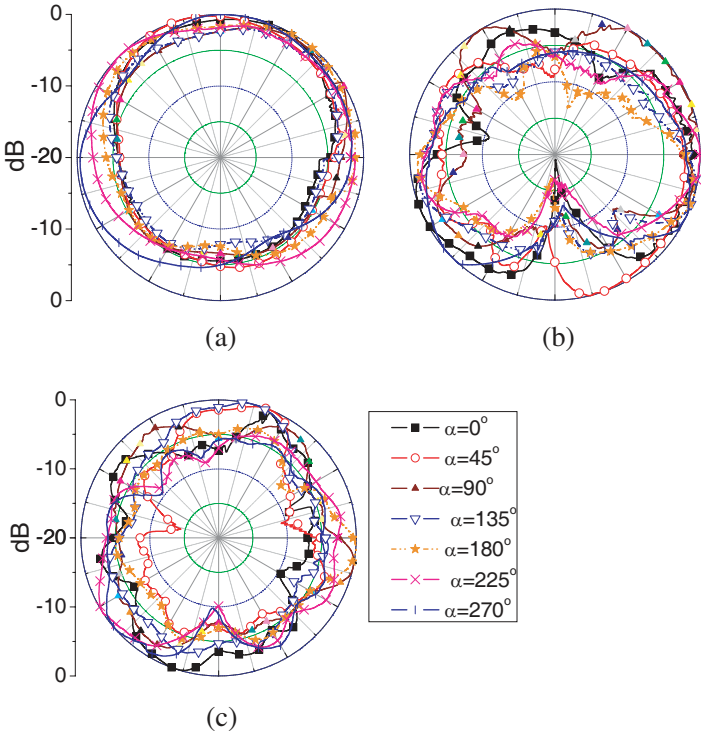

Figure 11. Curved conformal antennas' measured pattern in XY plane for the different curving angle α: (a) $f = 2.45\,\text{GHz}$; (b) $f = 5.25\,\text{GHz}$; (c) $f = 5.8\,\text{GHz}$.

4.3. Gain

The simulated and the measured gain for these curved antennae with different curving angle α at 2.45 GHz, 5.25 GHz and 5.8 GHz are listed in Table 7, and the measured gain is from 2 dBi to 6.3 dBi, and their varying trend is similar with the simulaton's.

5. CONCLUSION

The DGS is adopted in the ground design of the planar microstrip antenna to achieve the useful multiband, small size and gain enhancement, which is the basic of the curved conformal antenna, the relationship between the structure parameters and the antennas' characters are studied, which is the reference for the curved antenna.

With the curving angle α increasing, the return loss at $f = 2.45\,\text{GHz}$ almost keep good, but becomes poor at $f = 5.25\,\text{GHz}$ and 5.8 GHz. After slightly tuning the key parameters, these curved conformal antennas all can work well at $f = 2.45\,\text{GHz}$, 5.25 GHz and 5.8 GHz, and their patterns become more omni-directional with the curving angle α increasing, which are verified by experiment too. The measured gain of these antennas are 2 dBi to 6.3 dBi.

ACKNOWLEDGMENT

This work was supported by National Science Fund for Creative Research Groups (60821062), "973" project (2009CB320205) and National Science Fund (F010402/60501016) of China.

REFERENCES

1. He, W., R. Jin, J. Geng, and M. Lampe, "Multiband dual patch antennas with polarization compensation for WLAN applications," *Microwave and Optical Technology Letters*, Vol. 49, No. 8, 1907–1911, 2007.
2. He, W., R., Jin, J., Geng, and B. Gao, "Multiband antenna system with polarization conversion for wlan applications," *Microwave and Optical Technology Letters*, Vol. 49, No. 7, 1772–1777, 2007.
3. Raj, R. K., M. Joseph, B. Paul, and P. Mohanan, "Compact planar multiband antenna for GPS, DCS, 2.4–5.8 GHz WLAN applications," *Electronics Letters*, Vol. 41, No. 6, 290–291, 2005.
4. Zhong, Q., Y. Li, H. Jiang, and Y. Long, "Design of a novel dual-frequency microstrip patch antenna for WLAN applications," *Antennas and Propagation Society International Symposium, 2004. IEEE*, Vol. 1, 277–280, June 2004.
5. Archevapanich, T. and N. Anantrasirichai, "Inversed E-shape slot antenna for WLAN applications," *International Conference on Control, Automation and Systems 2007*, 2854–2857, COEX, Seoul, Korea, Oct. 17–20, 2007.
6. Janapsatya, J. and K. P. Esselle, "Multi-band WLAN antennas based on the principle of duality," *Antennas and Propagation Society International Symposium 2006, IEEE*, 2679–2682, 2006.
7. Wong, K.-L. and J.-S. Chen, "Cavity-model analysis of a slot-coupled cylindrical-rectangular microstrip antenna," *Microwave and Optical Technology Letters*, Vol. 9, No. 20, 124–127, 1995.
8. Chen J.-S. and K.-L. Wong, "Input impedance of a slot-coupled

cylindrical-circular microstrip patch antenna," *Microwave and Optical Technology Letters*, Vol. 11, No. 1, 21–24, 1996.

9. Dahele, J. S., R. J. Mitchell, K. M. Luk, and K. F. Lee, "Effect of curvature on characteristics of rectangular patch antenna," *Electron. Lett.*, Vol. 23, 748–749, 1987.
10. Yablonovitch, E., "Inhibited spontaneous emission in solid-state physics and electronics," *Phys. Rev. Lett.*, Vol. 58, 2059–2062, 1987.
11. Qu, D. and L. Shafai, "The performance of microstrip patch antennas over high impedance EBG substrates withinand outside its bandgap," *2005 IEEE International Symposium on Microwave, Antenna, Propagation and EMC Technologies for Wireless Communications Proceedings*, 423–426, 2005.
12. Jin, N., A. Yu, and X. Zhang, "An enhanced 2_2 antenna array based on a dumbbell EBG structure," *Microwave and Optical Technology Letters*, Vol. 39, 395–399, 2003.
13. He, W., R. Jin, and J. Geng "Low RCS and high performances of microstrip antenna using fractal UC-EBG ground," *IET Microwaves, Antennas and Propagation*, Vol. 1, No. 5, 986–991, 2007.
14. He, W., R. Jin, J. Geng, and G. Yang, "2×2 array with UC-EBG ground for low RCS and high gain," *Microwave and Optical Technology Letters*, Vol. 49, No. 6, 1418–1422, 2007.
15. Brown, E. B., C. D. Parker, and E. Yablonovitch, "Radiation properties of a planar antenna on a photonic-crystal substrate," *J. Opt. Soc. Am. B*, Vol. 10, No. 2, 404, 1993.
16. Radistic, V., Y. Qian, R. Cocciloli, et al., "Novel 2-D photonic bandgap structure for microstrip lines," *IEEE Microwave Guided Wave Letters*, Vol. 8, No. 2, 69, 1998.
17. Matttew, M. B., B. B. John, O. E. Henry, et al., "Two dimentional photonic crystals fabry-perror resonators with lossy dielectrics," *IEEE Trans. Microwave Theory Tech.*, Vol. 49, No. 11, 2085, 1999.
18. Qian, Y., D. Sievenpiper, V. Raisic, et al., "A novel approach for gain and bandwidth enhancement of patch antennas," *RAWON'98 Proceedings*, 221, 1998.
19. Wang, X., Y. Hao, and P. S. Hall, "Dual-band resonances of a patch antenna on UC-EBG substrate," *Asia-Pacific Microwave Conference Proceedings*, Vol. 1, 4–8, 2005.
20. Zulkifli, F. Y., E. T. Rahardjo, and D. Hartanto, "Radiation properties enhancement of triangular patch microstrip antenna array using hexagonal defected ground structure," *Progress In*

Electromagnetics Research M, Vol. 5, 101–109, 2008.

21. Lin, X.-C. and L.-T. Wang, "A wideband CPW-fed patch antenna with defective ground plane," *IEEE Antennas and Propagation Society International Symposium*, Vol. 4, 3717–3720, 2004.
22. Wong, K. L., J. S. Kuo, and T. W. Chiou, "Compact microstrip antennas with slots loaded in the ground plane," *Antennas and Propagation 11th International Conference*, Vol. 2, 623–626, Apr. 2001.
23. Lin, S.-Y. and K.-L. Wong, "Effects of slotted and photonic bandgap ground planes on the charaetsristics of an air-substrate annular-ring patch antenna at TM_{21} mode," *Proceeding of APMC 2001*, Vol. 2, 655–658, 2001.
24. Wang, L.-T. and J.-S. Sun, "The compact, broadband microstnp antenna with defective ground plane," *IEE International Conference on Antenna and Propagation*, Vol. 2, 622–624, Apr. 2003.
25. Liu, H., Z. Li, X. Sun, and J. Mao, "Harmonic suppression with photonic bandgap and defected ground structure for a microstrip patch antenna," *IEEE Microwave and Wireless Components Letters*, Vol. 15, No. 2, 55–56, 2005.
26. Guerin, N., C. Hafner, X. Cui, et al., "Compact directive antennas using frequency-selective surface (FSS)," *2005 Asia-Pacific Microwave Conference Proceedings*, Vol. 1, 519, 2005.
27. Richards, W., "An improved theory for microstrip patches," *IEE Proc. Part. H*, Vol. 132, 93–98, 1985.
28. Ansarizadeh, M. and A. Ghorbani, "An approach to equivalent circuit modeling of rectangular microstrip antennas," *Progress In Electromagnetics Research B*, Vol. 8, 77–86, 2008.
29. Abboud, F., J. P. Damiano, and A. Papiernik, "Simple model for the input impedance of coax-fed rectangular microstrip patch antenna for CAD," *Microwaves, Antennas and Propagation, IEE Proceedings H*, Vol. 135, No. 5, 323–326, 1988.
30. Park, J.-S., "An equivalent circuit and modeling method for defected ground structure and its application to the design of microwave circuits," *Microwave Journal*, Vol. 46, No. 11, 22–38, Nov. 2003.
31. Hai, S., H. Guang, and H. Wei, "A broadband dual-polarized triangle patch antenna with DGS," *Journal of Microwaves*, Vo1. 21, No. 4, 27–30, Aug. 2005 (in Chinese).
32. http:\\www.cst.de\Content\Company\Academic.aspx.
33. Weiland, T., "Time domain electromagnetic field computation

with finite difference methods," *International Journal of Numerical Modelling: Electronic Networks, Devices and Fields*, Vol. 9, No. 4, 259–319, Dec. 1998.

34. Geng, J., R. Jin, W. Wang, W. He, M. Ding, Q. Wu, X. Rui, G. Yang, and Z. Fang, "A new quasi-omnidirectional vertical polarisation antenna with low profile and high gain for DTV on vehicle," *Microwaves, Antennas & Propagation, IET*, Vol. 1, No. 4, 918–924, Aug. 2007.